23rdABCM International Congress of Mechanical Engineering
December 6-11, 2015, Rio de Janeiro, RJ, Brazil

ANALYSIS OF HYGROTHERMAL PERFORMANCE AND MOULD GROWTH ON CONCRETE TILES

Gerson Henrique dos Santos
Federal Technological University of Paraná– UTFPR
Mechanical Engineering Graduate Program – 84016-260 – Ponta Grossa, Brazil
gsantos@utfpr.edu.br

Nathan Mendes
Pontifical Catholic University of Paraná - PUCPR
Mechanical Engineering Graduate Program – 80215-901 – Curitiba, Brazil
nathan.mendes@pucpr.br

Abstract. *Roofs play an important role on energy consumption and thermal comfort, especially in low-rise buildings. In this context, the use of cool roofs can reduce energy consumption by decreasing air conditioning needs, improving indoor thermal comfort and extend roof service life. However, after long service life, the solar absorptivity coatings can be increased due to mold or algae growth, decreasing their thermal performance. Therefore, a mathematical model considering the combined two-dimensional heat, air and moisture transport through an unsaturated roof is presented. The differential governing equations are based on driving potentials of temperature, moist air pressure and water vapor pressure gradients. In the results section, the effects of moisture adsorption and desorption on the thermal performance of concrete tiles due to an additional transport mechanism is shown and a well-known model for predicting mould growth is applied illustrating a risk index.*

Keywords: *concrete tiles, hygrothermal performance, mould growth.*

1. INTRODUCTION

The worldwide energy consumption to obtain indoor thermal comfort in buildings has been continuously growing. In Brazil, residential and commercial buildings are responsible for about 45% of the total consumption of electricity, which progressively motivates energy conservation studies for promoting building energy efficiency. In this context, the cost of heating and cooling of buildings is directly affected by roofs performance. The use of insulating or a higher roof solar reflectance reduces the solar energy absorbed by the roof and therefore usually provides a reduction in the cost of air conditioning in warmer climate countries.

In this context, reflective roof or insulation coatings have been utilized for increasing the energy savings potential of building envelope and several research work can be found in the literature such as Al-Sanea (2002), Suehrcke *et al.* (2008), Belusko *et al.* (2011), Saber *et al.* (2012) and D'Orazio *et al.* (2012). However, due to the low cost, concrete or ceramic tiles are widely used in roofs in Brazil. Those tiles enable the mould or algae to grow and normally no pain or impermeable films (Fig. 1) are provided. In asphalt roofing shingles found widely in European and North American buildings, this phenomenon is commonly observed (Fig. 2). The mould growth decreases the tiles durability, worsens the aesthetic appearance of buildings and increases the solar absorptivity.

Figure 1. Mould Growth on concrete tiles.

Figure 2. Mould growth on asphalt roofing shingles.

Regarding mould prediction models and their influence on mould risk assessment, some models can be found in the literature (Vereecken and Roels, 2012). Hukka and Viitannen (1999) developed a model based on the relative humidity and temperature that allows determining the temporal development of the mould growth. First, the original model was based on the work with untreated pine and spruce sapwood. Viitannen *et al.* (2011) improved that model during a joint project carried out at VTT (Technical Research Center of Finland) and at Tampere University of Technology. This project large sets of steady-state and dynamic laboratory experiments for different buildings materials were carried out. In their study presented in the literature, the mould growth prediction and the analysis including the combined heat and mass transport through roofing systems composed of concrete tiles and timber rafters is barely explored. However, it is well known nowadays, that a fully coupled multidimensional model is necessary to study the impact of moisture on the building hygrothermal performance and on durability aspects.

In this way, a mathematical model considering the combined two-dimensional heat, air and moisture transport through unsaturated porous elements to analyze the hygrothermal performance of concrete tiles is presented. The model is based on driving potentials of temperature, air pressure and water vapor pressure gradients for consolidated porous materials. The solution of the sets of governing equations has been simultaneously obtained using the MTDMA (MultiTriDiagonal-Matrix Algorithm) for the three potentials, avoiding numerical divergence caused by the evaluation of coupled terms from previous iteration values. In the results section, comparisons in terms of heat fluxes at the internal boundary as well as the mould growth risk are presented and discussed.

2. MATHEMATICAL MODEL

The model for the porous media domain (Fig. 3) has been elaborated considering the differential governing equations for moisture, air and energy balances. The transient terms of each governing equation have been written in terms of the driving potentials to take more advantage of the MTDMA (Mendes *et al.*, 2002) solution algorithm.

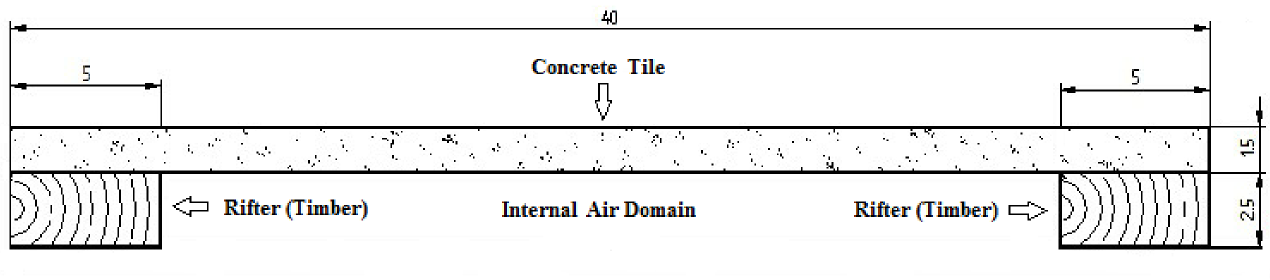

Figure 3. Physical domain and dimensions (cm) of the roof.

2.1 Porous Element Domain

The model is based on averages taken over a representative elementary volume (REV). The moisture transport has been divided into liquid and vapor flows as shown in Eq. 1:

$$\mathbf{j} = \mathbf{j}_l + \mathbf{j}_v \, , \tag{1}$$

where $\mathbf{j}$ is the density of moisture flow rate (kg/m²s), $\mathbf{j_l}$, the density of liquid flow rate (kg/m²s) and, $\mathbf{j_v}$, the density of vapor flow rate (kg/m²s). The liquid transport calculation is based on the Darcy equation:

$$\mathbf{j_l} = K(\nabla P_{suc} - \rho_l \mathbf{g}), \tag{2}$$

where K is the liquid water permeability (s), P_{suc}, the suction pressure (Pa), ρ_l, the liquid water density (kg/m³) and $\mathbf{g}$ the gravity (m/s²).

The capillary suction pressure can be written as a function of temperature and moisture content in the following form:

$$\nabla P_{suc} = \frac{\partial P_{suc}}{\partial T}\nabla T + \frac{\partial P_{suc}}{\partial P_v}\nabla P_v. \tag{3}$$

Similarly to the liquid flow, the vapor flow is calculated from the Fick equation considering effects of both vapor pressure and air pressure driving potentials:

$$\mathbf{j_v} = -\underbrace{\delta_v \nabla P_v}_{\substack{vapor \\ diffusion}} - \underbrace{\rho_v \frac{k k_{rg}}{\mu_g}\nabla P_g}_{\substack{\text{vapor} \\ \text{advection}}}, \tag{4}$$

where δ_v is the vapor diffusive permeability (s), P_v, the partial vapor pressure (Pa), ρ_v, the vapor density (kg/m³), k, the absolute permeability (m^2), k_{rg}, the gas relative permeability, μ_g, the dynamic viscosity (Pa.s) and, P_g, the gas pressure. The water mass conservation equation can be described as:

$$\frac{\partial w}{\partial t} = -\nabla.\mathbf{j}, \tag{5}$$

where w is the moisture content (kg/m³).

This moisture content conservation equation – Eq. 5 – can be written in terms of the three driving potentials as:

$$\frac{\partial w}{\partial \phi}\frac{\partial \phi}{\partial P_v}\frac{\partial P_v}{\partial t} + \frac{\partial w}{\partial \phi}\frac{\partial \phi}{\partial T}\frac{\partial T}{\partial t} = \nabla.\left[-K\frac{\partial P_{suc}}{\partial T}\nabla T - \left(K\frac{\partial P_{suc}}{\partial P_v} - \delta_v\right)\nabla P_v + \rho_v \frac{k k_{rg}}{\mu_g}\nabla P_g + K\rho_l \mathbf{g}\right]. \tag{6}$$

In the proposal model, the air transport is individually considered through the dry-air mass balance. In this way, the dry-air conservation equation can be expressed as:

$$\frac{\partial \rho_a}{\partial t} = -\nabla.\mathbf{j}_a, \tag{7}$$

with the air flow calculated by the following expression:

$$\mathbf{j}_a = \underbrace{\delta_v \nabla P_v}_{air\ diffusion} - \underbrace{\rho_a \frac{k k_{rg}}{\mu_g}\nabla P_g}_{air\ convection}, \tag{8}$$

where ρ_a is the dry-air density (kg/m^3), $\mathbf{j}_a$, the dry-air flow rate density (kg/m²s) and, P_g, the gas pressure (dry air pressure plus vapor pressure, in Pa). Therefore, the dry air transport can be described as a function of the partial gas and vapor pressure driving potentials so that the air balance can be written as:

$$\frac{\partial \rho_a}{\partial P_g}\frac{\partial P_g}{\partial t}+\frac{\partial \rho_a}{\partial P_v}\frac{\partial P_v}{\partial t}+\frac{\partial \rho_a}{\partial T}\frac{\partial T}{\partial t}=\nabla.\left(-\delta_v \nabla P_v+\rho_a\frac{kk_{rg}}{\mu_g}\nabla P_g\right). \tag{9}$$

Due to the presence of low temperature gradients, heat transfer has been attributed to both conductive and convective effects only. The conductive transport is calculated by the Fourier's law:

$$\mathbf{q}_{\mathbf{cond}}=-\lambda \nabla T\ , \tag{10}$$

while the convective transport can be written as:

$$\mathbf{q}_{\mathbf{conv}}=\underbrace{\mathbf{j}_{\mathbf{l}} c_{pl} T}_{liquid\ flow}+\underbrace{\mathbf{j}_{\mathbf{a}} c_{pa} T}_{dry air\ \text{flow}}+\underbrace{\mathbf{j}_{\mathbf{v}} L}_{\substack{phase\\ change}}+\underbrace{\mathbf{j}_{\mathbf{v}} c_{pv} T}_{vapor\ \text{flow}}\ , \tag{11}$$

where λ is the thermal conductivity (W/mK), c_{pa}, the dry-air specific heat at constant pressure (J/kgK), c_{pl}, the liquid water specific heat (J/kgK), c_{pv}, the vapor specific heat at constant pressure of the (J/kgK) and, L, the vaporization latent heat (J/kg).

The energy balance equation based on the 1st law of thermodynamics can be written in this case as:

$$c_m\rho_0\frac{\partial T}{\partial t}=-\nabla.\mathbf{q}\ , \tag{12}$$

where c_m is the specific heat of the structure (J/kgK) and ρ_0, the dry-basis material density (kg/m³). In this way, assuming 0°C as the reference temperature, the energy conservation equation can be rewritten in terms of the three driving potentials as:

$$c_m\rho_0\frac{\partial T}{\partial t}=\nabla.\left(\begin{aligned}&\left(\lambda-K\frac{\partial P_{suc}}{\partial T}c_{pl}T\right)\nabla T-\left(K\frac{\partial P_{suc}}{\partial P_v}c_{pl}T+\delta_v c_{pa}T-\delta_v\left(L+c_{pv}T\right)\right)\nabla P_v+\\&\left(\rho_a\frac{kk_{rg}}{\mu_g}c_{pa}T+\rho_v\frac{kk_{rg}}{\mu_g}\left(L+c_{pv}T\right)\right)\nabla P_g+K\rho_l c_{pl}T\mathbf{g}\end{aligned}\right). \tag{13}$$

2.2 Mould Growth Model

The mould growth prediction has been verified through of the model presented by Viitannen *et al.* (2011). The mould has been measured applying an existing standard index based on the visual appearance of the surface under study. This mould index assumes the following values:

0 - no growth;
1 - some growth detected only with microscopy;
2 - moderate growth detected with microscopy (coverage more than 10%);
3 - some growth detected visually;
4 - visually detected coverage more than 10%;
5 - visually detected coverage more than 50%;
6 - visually detected coverage 100%.

The index M is presumed to increase linearly in time:

$$\frac{dM}{dt} = \frac{1}{7e^{(-0.68\ln T - 13.9\ln RH + 0.14W - 0.33SQ + 66.02)}} k_1 k_2, \tag{14}$$

where k_1 represents the intensity of growth, k_2 is the moderation of the growth intensity when the mould index (*M*) level approaches the maximum peak value, *W* is the timber species (0 = pine and 1 = spruce) and *SQ* is the term for surface quality (*SQ* = 0 for sawn surface, *SQ* = 1 for kiln dried quality), *T* is the temperature (° C) and *RH*, the relative humidity (%). The terms k_1 and k_2 are modified for other materials than wood and *SQ* = 0 is used. The idea is to compare the mould growth of other materials to that of the pine sapwood (original work). More details can be seen in Viitannen *et al.* (2011).

3. SIMULATION PROCEDURE

The roof analyzed is composed of concrete tile (1.5 cm) and two rifters (2.5 cm) as shown in Fig. 3. The hygrothermal properties have been obtained from Künzel *et al.* (2008) for concrete and from IEA Annex 14 Report (IEA, 1991) for timber (rifters). The internal emissivity was considered equal to 0.9 for both concrete tile and timber roofs.

A regular 2-D mesh (2.5 mm²) for the discretization using the finite-volume method and a 30-s constant time step have been applied for all simulations.

The outdoor conditions were represented by the TRY (Test Reference Year) weather data for the city of Curitiba-Brazil. Constant convective heat transfer coefficients of 3 and 10 W/m²K have been used at the internal and external surfaces. The external and internal convective water vapor transfer coefficients are calculated by the Lewis's relation for each control volume. The other surfaces were considered adiabatic and impermeable. The Swinbank (1963) sky temperature correlation has been used in this work. Gas (moist air) pressure has been considered constant at all surfaces.

4. RESULTS

Heat fluxes at the internal roof surfaces are presented in Fig. 4. The mass transport effect is verified when a roof was simulated without the moisture content and air conservation equations. As observed in Fig. 4, the latent effect was small when compared with the sensible heat flux. This fact is attributed to period analyzed (January). This effect is increased in the winter (not shown), where the sensible heat flux loses dramatically its magnitude and the Sun does not dry out the roof as it does in the summer. However, a difference of 20 % on the heat flux is reported for the peak values when the mass transport is considered.

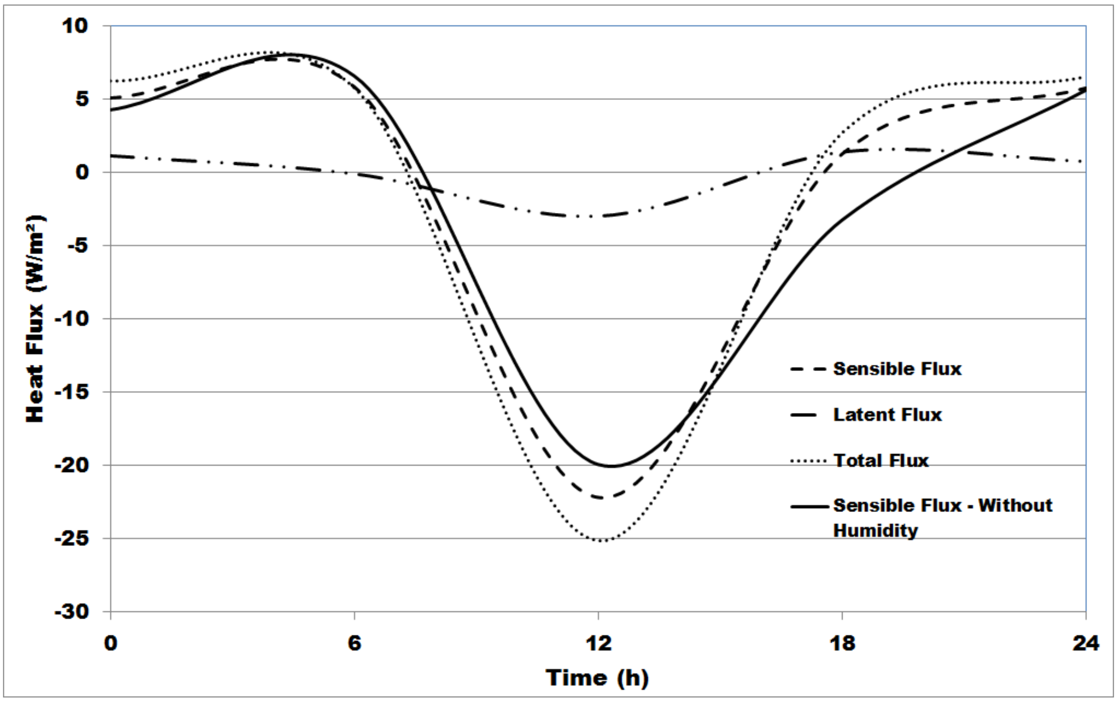

Figure 4.Heat fluxes at the internal roof surface on January 7th.

Figure 5 presents the temperature and relative humidity profiles within the roof at midnight on January 7th. The low temperature at the external surface increases the relative humidity and, consequently, the mould index in this period, as described by Eq. 14. Although the indoor latent heat flux is small when compared to the sensible flux, the mass transport can play an important role on the heat exchanged at the external surface, mainly, at daytime, when the adsorbed moisture at nighttime (Fig. 7) is released, decreasing the concrete tile temperature due to the outward evaporation.

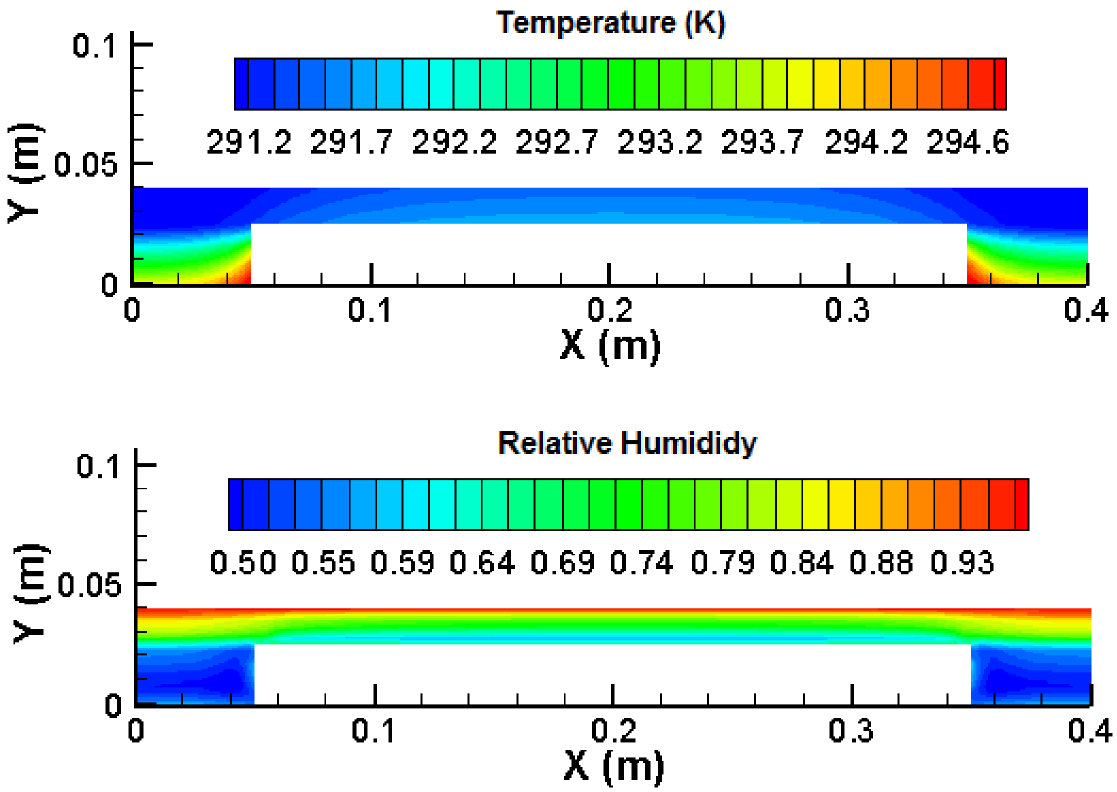

Figure 5. Temperature (K) and relative humidity profiles in the roof at midnight on January 7th.

The mould index evolution is reported in Fig. 6. Some mould growth can be detected visually after 76 weeks (Curitiba climate). A small decrease in the mould index also is observed after the winter period. This work has been limited to 85 weeks due to the high computational time required and to the fact that according to the VVT model mould would visually appear in less than 85 weeks..

Beyond damages and the roof appearance, the mould growth can change the solar absorptance of the external roof surface, causing a high building thermal load. The results indicate that a cleaning preventive maintenance is suggested every two years. This problem can be mitigated by using impermeable coating on the tiles.

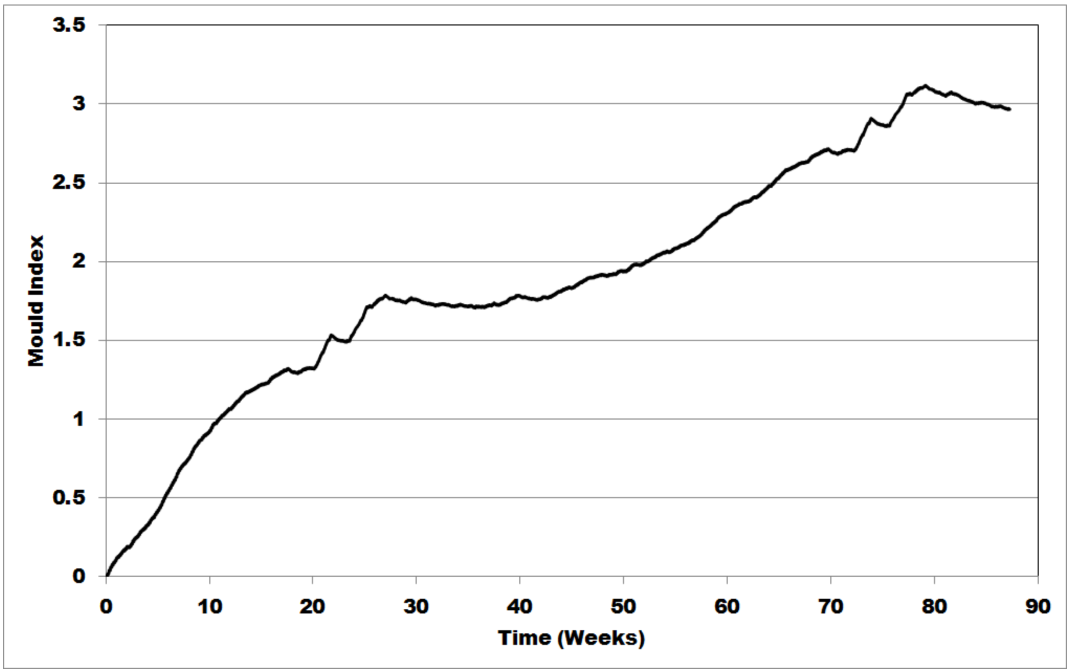

Figure 6. Mould index evolution in the concrete tile.

5. CONCLUSIONS

Roofs are submitted to both thermal and moisture gradients so that an accurate heat transfer determination requires a simultaneous calculation of both sensible and latent effects. Therefore, a mathematical model considering the combined two-dimensional heat, air and moisture transport through unsaturated roof was presented and the effects of moisture adsorption and desorption on the thermal performance of concrete tiles was shown.

Besides its effect on heat transfer, moisture can cause damage to the building structure and can promote the growth of mould and mildew. The mould growth on roof surfaces can increase the solar absorptivity, decreasing its hygrothermal performance.

For future work, we intend to include the changes on roof solar absorptivity in the presented model, so that mould growth and the effects on the hygrothermal performance of the building could be verified more precisely.

6. REFERENCES

Al-Sanea,S. A., 2002.Thermal performance of building roof elements. Building and Environment, 37, pp. 665–675.

Belusko, M., Bruno, F., Saman, W., 2011. Investigation of the thermal resistance of timber attic spaces with reflective foil and bulk insulation, heat flow up. Applied Energy, 88, pp. 127–137.

D'Orazio, M., Di Perna, C., Di Giuseppe, E., Morodo, M., 2012.Thermal Performance of an insulated roof with reflective insulation: Field tests under hot climatic conditions, Journal of Building Physics, 36(3), pp. 229–246.

Hukka, A., Viitanen, H. A., 1999. A Mathematical Modelof Mould Growth on Wooden Material.Wood Science and Technology, 33, pp. 475-485.

IEA - Annex XIV : Condensation and Energy - Catalogue of Material Properties, 1991, Vol. 3.

Künzel, H. M., Holm, A. H., Krus, M., 2008. Hygrothermal Properties and Behaviour of concrete. WTA-Almanach, pp. 161-181.

Mendes, N., Philippi, P. C., Lamberts, R., 2002. A New Mathematical Method to Solve Highly Coupled Equations of Heat and Mass Transfer in Porous Media. International Journal of Heat and Mass Transfer, 45, pp. 509-518.

Saber, H. S.,Maref, W.,Sherrer, G., Swinton, M. C., 2012.Numerical modeling and experimental investigations of thermal performance of reflective insulations.Journal of Building Physics. 36(2), pp. 163–177.

Suehrcke,H., Peterson, E. L., Selby, N., 2008.Effect of roof solar reflectance on the building heat gain in a hot climate. Energy and Buildings, 40, pp. 2224–2235.

SwinBank, W. C., 1963. Long wave radiation from clear skies.Quart. J. Roy. Meteorol.Soc., 89.

Vereecken, E., Roels, S., 2012. Review of Mould Prediction Models and their Influence on Mould Risk Evaluation. Building and Enviromment, 51, pp. 296-310.

Viitanen, H. A., et. al., 2011.Mould Growth Modelling to Evaluate Durability of Materials. International Conference on Durability of Building Materials and Components, Porto, Purtugal.

7. RESPONSIBILITY NOTICE

The authors are the only responsible for the printed material included in this paper.